Tokamak experiments in RFX-mod with polarized insertable electrode

L.Carraro, R.Cavazzana, S.Dal Bello, G. De Masi, A.Ferro, C.Finotti, P.Franz, L.Grando, P.Innocente, O.Kudlacek, G.Marchiori, L.Marrelli, E.Martines, R.Paccagnella, P.Piovesan, C.Piron, M.E.Puiatti, M.Recchia, P.Scarin, S.Spagnolo, M.Spolaore, C.Taliercio, B.Zaniol, L.Zanotto, M.Zuin

[1] *Consorzio RFX, Euratom/ENEA Association, Padova, Italy*

Introduction: The RFX-mod device (R=2m, a=0.459m) can be operated as an ohmic tokamak with a toroidal field up to 0.55T for 1.5 sec, using deuterium as filling gas. Thanks to its MHD control system and to the close fitting vacuum vessel, it can systematically operate circular cross section discharges up to very low q regimes[1] (q(a)<2). Moreover, taking advantage of its flexible system of power supplies and field shaping windings, discharges with non-circular cross section have been realized[2,3]. This paper reports about enhanced confinement regimes, obtained both in circular and single null (SN) tokamak discharges, with an insertable polarized graphite electrode.

Experimental Setup: The electrode head consists of a graphite truncated ellipsoid (115x37x64 mm). It is connected to a manipulator and inserted inside the plasma from an access located on the lower part of the device. Depending on the plasma position and shape, the tip of the electrode has been inserted from 2.5cm up to 8cm inside the Last Closed Flux Surface. The electrode has been fed using one of the main power supplies of the machine, a single quadrant 12-pulse regulated bridge[4]. An LR network is used to filter the fire sequence of the thyristors as shown in Fig. 1 (1.67 ms period). To preserve the electrode from damages, the electrode power supply was controlled through the MARTe real-time control system of RFX, programmed to turn off the power supply when the $I_{el}V_{el}$ curve was out of the expected range (i.e. due to an arc). The temperature of the electrode was monitored by an infrared camera in order to avoid overheating. The applied electrode voltage ranged from -800V to +350V with currents up to 300A: the I,V characteristic curve for a set of similar SN discharges is shown in Fig 2:

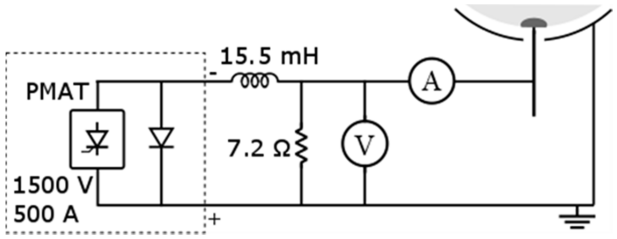

Fig. 1) Power supply schematics

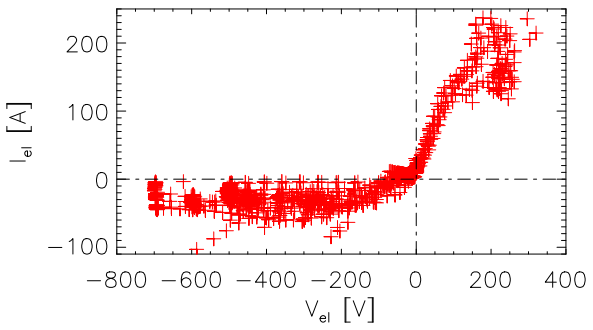

Fig. 2) Electrode I,V characteristic curve.

each point corresponds to an average over 10ms. Circular plasmas features are a=42-45cm, I_p=60-95kA, q(a)=2.7-4, n_e up to 8 $10^{18}m^{-3}$. Circular discharges are operated with a 0.5-1cm horizontal displacement towards the high field side: the inner first wall therefore acts as a toroidal limiter. Single null (SN) discharges are somewhat smaller, a=36-39cm (X-point distance from the first wall 0.5-2 cm), I_p=45-75kA, q_{95}= 2.5-4.5, n_e up to 5 $10^{18}m^{-3}$. Edge polarization has also been tested in a few circular q(a)<2 discharges at I_p=140kA: decreased D_α and increased density have been observed but difficult density control and frequent disruptions did not allow a systematic exploration within the available experimental time.

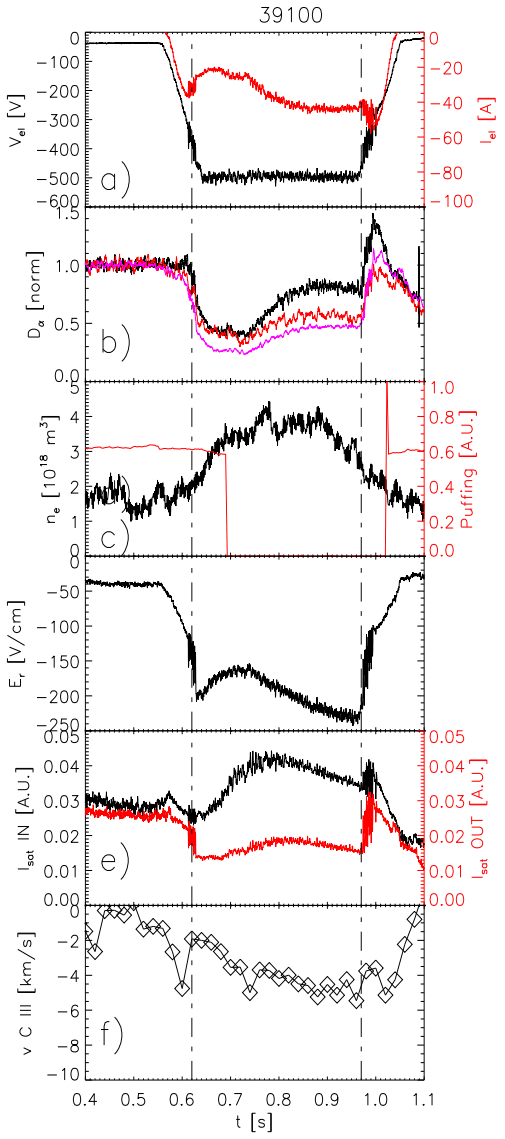

Fig. 3) Transition to high confinement example. See text for captions.

Transitions to enhanced confinement: both limiter and SN discharges are characterized by transitions to high confinement when the electrode is negatively polarized with respect to the first wall. The negative polarization follows the spontaneous polarization feature of the plasma without biasing. An example is shown for a Single Null discharge, shot 39100, in Fig. 3, and a similar behavior is found for circular limiter discharges. When the applied voltage V_{el} (panel a:black trace) exceeds a threshold value (approximately around 200-300V for the experiments performed so far) and the electron density is sufficiently high, the electrode current suddenly decreases (a-red trace): between 0.6s and 0.95s in this example; D_α signals, measured along different lines of sights, abruptly decrease (b); the electron density increases even if puffing valve reference (b-red trace) is set to 0 by the feedback system[5] (c); similarly, the poloidal beta and the diamagnetic energy also increase. The inward pointing electric field (d) is estimated as the difference of the floating potential measured by two neighbor probes located across the LCFS, on the same poloidal and toroidal

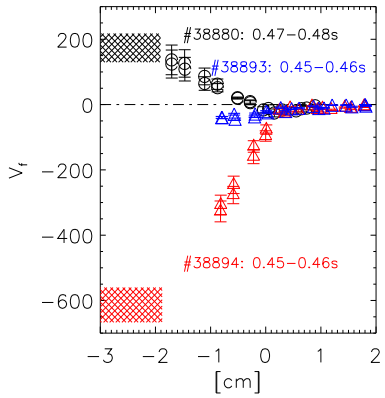

Fig 4) Floating potential profiles. Shaded areas represent electrode voltage and distance from LCFS

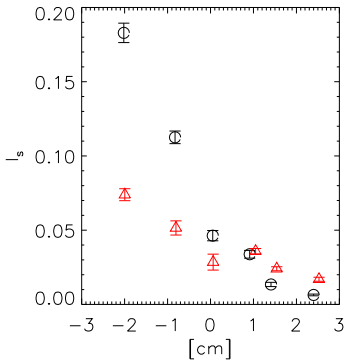

Fig. 5) a)V_f and b) I_s profiles (red before and black during transition.

position through the U-probe insertable probe system [6]; it varies proportionally to the electrode voltage and it becomes more negative after the transition is established. The saturation current (which is proportional to electron density) of probes located outside the separatrix suddenly decreases (e-red trace), while the signal of an innermost probe remains unchanged at first and then increases (e-black trace): this indicates a steepening of the edge electron density profile. The spectroscopically determined toroidal flow of CIII (f), an ion species located in the edge region, becomes more negative (plasma current and toroidal field being both directed in the positive toroidal direction) as soon as the electrode is polarized: this acceleration is parallel to the J_r x B_θ force (J_r is directed inward).

Positive polarization has been attempted both in circular and SN discharges. As the electrode behaves approximately like a Langmuir probe, higher currents are drawn, frequently leading to intervention of the electrode protection system. Even though density and diamagnetic energy increase, D_α decreases, in this case, only for very short (few ms) time intervals.

The floating potential as a function of the distance from LCFS (indicative of the radial electric field behavior) varies according to the polarization of the electrode as can be seen in Fig. 4) showing that a strong electric fields builds up in the few cm region within the LCFS: blue symbols represent the naturally negative floating potential when the electrode is not inserted. The radial profile of saturation current (Fig 5) steepens during transitions (black symbols) compared to before transition phase (red symbols): this indicates that a local transport barrier is established, sustained by the polarized electrode.

Dithering behavior: Depending on experimental conditions, periodic back transitions to low confinement mode can occur with different periods, ranging from 10-15ms (Fig. 6a) down to the power supply switching period of 1.5ms (Fig 6b). The dithering behavior can be observed both in circular and in SN discharges.

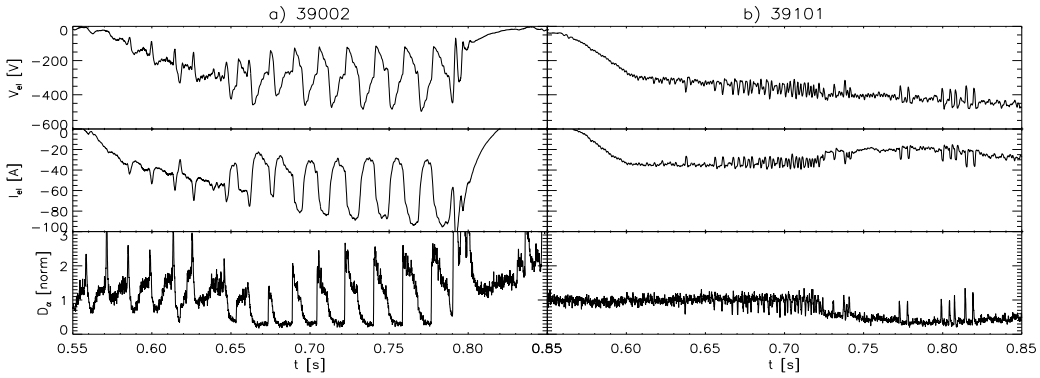

Fig. 6) Examples of dithering dynamics.

Dithering behavior is almost always observed during the electrode ramp-up or ramp-down when the voltage is near the threshold (the slower the voltage ramp the longer the dithering phase, similarly to the phenomenology described by the dithering model of Zohm et al.[7]); a number of intermittent fast events can also occur once the transition is well established (as in Fig 6b after 0.75s). Conditional averaging of ion saturation current (red trace) and a floating potential (black) inside the separatrix for a series of these fast events is shown in Fig. 7: the time is synchronized with respect to the D_α spike (blue trace). The reduction of V_f, and consequently of the radial electric field and its shear, occurs earlier then the decrease of the density gradient. This is consistent with the observation of the causal relationship between ∇E_r and ∇n_E reported in TEXTOR[8].

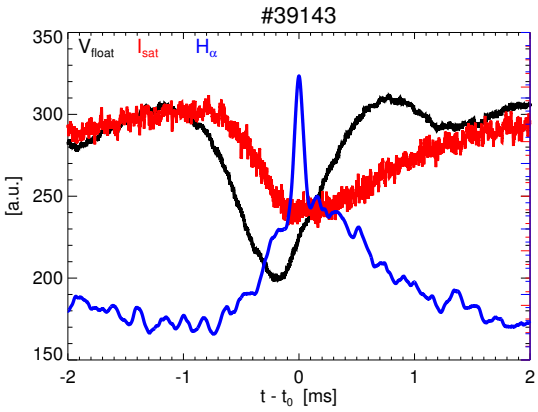

Fig. 7) Conditional average of V_f and I_s, with respect to the peak of H_α radiation

Summary: Transitions to enhanced confinement have been obtained in RFX-mod tokamak circular and SN discharges showing a qualitatively similar behavior. Further analyses are in progress in order to highlight differences among the two configurations and to characterize in detail the characteristics of the fast dithering events.

[1] Zanca P. et al., Plasma Phys. Contr. Fusion 54(2012) 094004
[2] G.Marchiori, et al., 41st EPS Conference on Plasma Physics, (2014), P5.040
[3] Kudlacek O., et al., Physics of Plasmas 22, 102503 (2015)
[4] Maschio A. et al, Fusion Eng. Des 25 (1995), 401
[5] R.Cavazzana, et. al., 20th IEEE-NPSS Real Time Conf., submitted to IEEE T. Nucl. Science
[6] Spolaore M., et al., . 2009 J. Nucl. Mater. 390 448–51
[7] H.Zohm, et al., Phys. Rev. Lett., 72 (1994) 222
[8] Van Oost, et al., Plas. Phys. Contr. Fus. 45 (2003) 621